Open Archive Toulouse Archive Ouverte (OATAO)

OATAO is an open access repository that collects the work of Toulouse researchers and makes it freely available over the web where possible.

Ac conductivity and dielectric properties of $CuFe_{1-x}Cr_xO_2$: Mg delafossite

M Lalanne, P Demont and A Barnabé

Institut Carnot CIRIMAT, Université de Toulouse UPS, 118 Route de Narbonne, 31062, Toulouse cedex 9 France

E-mail: demont@cict.fr

Abstract
The electrical and dielectric properties of $CuFe_{1-x}Cr_xO_2$ ($0 \leqslant x \leqslant 1$) powders, doped with 3% of Mg and prepared by solid-state reaction, were studied by broadband dielectric spectroscopy in the temperature range from -100 to $150\,°C$. The frequency-dependent electrical and dielectric data have been discussed in the framework of a power law conductivity and complex impedance and dielectric modulus. At room temperature, the ac conductivity behaviour is characteristic of the charge transport in $CuFe_{1-x}Cr_xO_2$ powders. The substitution of Fe^{3+} by Cr^{3+} results in an increase in dc conductivity and a decrease in the Cu^+–Cu^+ distance. Dc conductivity, characteristic onset frequency and Havriliak–Negami characteristics relaxation times are thermally activated above $-40\,°C$ for $x = 0.835$. The associated activation energies obtained from dc and ac conductivity and from impedance and modulus losses are similar and show that $CuFe_{1-x}Cr_xO_2$ delafossite powders satisfy the BNN relation. Dc and ac conductivities have the same transport mechanism, namely thermally activated nearest neighbour hopping and tunnelling hopping above and below $-40\,°C$, respectively.

1. Introduction

For more than 30 years, delafossite compounds have been studied for their unusual magnetic and electrical properties [1–3]. More recently, delafossite compounds have attracted much attention since Kawazoe *et al* [4] showed that $CuAlO_2$ was a good candidate for p-type transparent conducting oxides (TCO). The development of p-type TCO is one of the most crucial technologies for p–n junction-based devices such as transparent solar cells and transparent light-emitting diodes. Among various materials, copper metal oxide with the molar ratio $Cu/M = 1$, i.e. $CuMO_2$, with $M = \{Al, Ga, Cr, \dots\}$ and with a delafossite structure has been known as one of the p-type TCO materials for potential industrial applications. Several $CuMO_2$ thin films have been reported with different conductivities and transparencies [5–9].

The $CuMO_2$ structure can be described as a stacking, along the c-axis, of edge-shared MO_6 octahedra forming MO_2 layers. These MO_2 layers are connected together with triangular metallic planes of monovalent copper. Each Cu^+ cation is linearly coordinated with two O^{2-} anions of upper and lower MO_2 layers as seen in figure 1. The oxygen layers can be stacked in different ways along the c-axis, leading to two polytypes of the delafossite structure: the hexagonal 2H (space group P6₃/mmc) and the rhombohedral 3R (space group R-3m) polytypes.

$CuFeO_2$ delafossite is a well-known p-type semiconductor. At room temperature, the highest electrical conductivity ($\sigma_{RT} = 2\,S\,cm^{-1}$) [1, 10] among the $CuMO_2$ delafossite series is obtained with p-type $CuFeO_2$ delafossite when an off-stoichiometric $CuFeO_{2+\delta}$ phase is formed. This electrical conductivity can also be improved by magnesium doping up to $30\,S\,cm^{-1}$ for $CuFe_{0.98}Mg_{0.02}O_2$ [10, 11]. In the $CuMO_2$ compounds, the transport properties are mainly governed by the copper mixed valency Cu^I/Cu^{II} [12, 13]. In $CuFeO_{2+\delta}$ and $CuFe_{1-x}Mg_xO_2$, this Cu^I/Cu^{II} ratio is, respectively, controlled by the oxygen non-stoichiometry value δ according to $(Cu^+_{1-2\delta}Cu^{2+}_{2\delta})FeO_{2+\delta}$ [14], and the Fe-site doping stoichiometry x according to $(Cu^+_{1-x}Cu^{2+}_x)(Cr^{3+}_{1-x}Mg^{2+}_x)O_2$. Moreover, $CuFeO_2$ can be deposited in thin film form by the radio-frequency sputtering method at low temperature on conventional glass [15], and then accordingly presents a real interest for industrial applications.

$CuCrO_2$ delafossite is also a p-type semiconductor but with a lower intrinsic electrical conductivity ($\sigma_{RT} = 3.5 \times 10^{-5}\,S\,cm^{-1}$) [9] due to the difficulties in intercalating oxygen
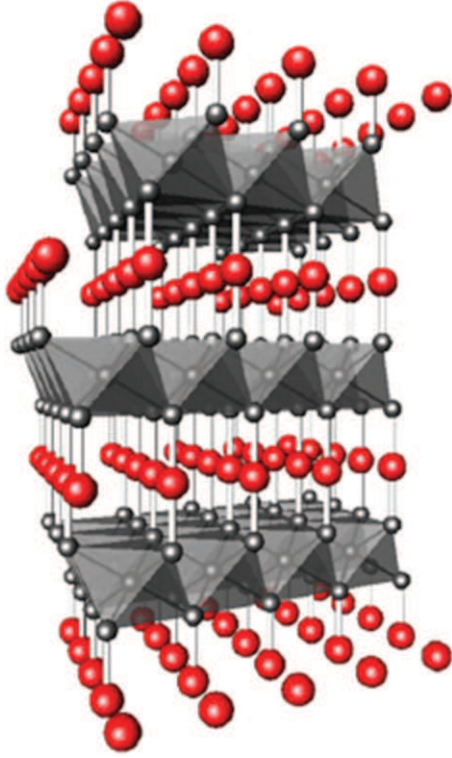
Figure 1. CuMO$_2$ delafossite structure.
(This figure is in colour only in the electronic version)

Figure 2. Angular frequency dependence of the real part σ' of the complex conductivity at room temperature (25 °C) for different x: (■) $x = 0$; (○) $x = 0.165$; (▲) $x = 0.333$; (∗) $x = 0.5$; (◇) $x = 0.667$; (▼) $x = 0.835$; (☆) $x = 1$. The solid lines represent the fit of experimental data using (1). The inset represents the x dependence of exponent n.

into the stoichiometric delafossite structure [16]. However, the electrical conductivity can also be improved up to 220 S cm^{-1} with appropriate M-site doping as in CuCr$_{0.95}$Mg$_{0.05}$O$_2$ thin film [8], by the same way as with CuFeO$_2$.
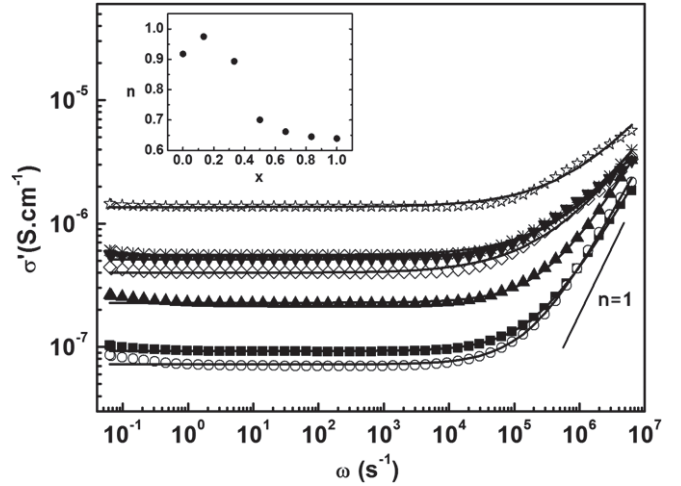
As a result, CuFe$_{1-x}$Cr$_x$O$_2$: Mg solid solution is particularly attractive due to the potential merge of the low temperature deposition process of the p-type CuFeO$_2$ delafossite and the optimized p-type TCO properties of CuCrO$_2$: Mg.

Previously, we studied the phase stability and thermal behaviour of the CuFe$_{1-x}$Cr$_x$O$_2$ ($0 \leqslant x \leqslant 1$) solid solution by thermogravimetric analysis (TGA) and high-temperature XRD under an air atmosphere up to 1000 °C in order to characterize the oxygen intercalation [16]. For $0 \leqslant x < 1$, two oxidations were observed. A slight oxidation appears between 400 and 500 °C, leading oxygen intercalation in the Cu$^+$ layers. An off-stoichiometric (Cu$_{1-2\delta}^+$Cu$_{2\delta}^{2+}$)Fe$_{1-x}$Cr$_x$O$_{2+\delta}$ delafossite phase is then formed. Above 500 °C, a phase transition occurs; the delafossite phase is transformed into spinel and CuO phases. For $x = 1$, i.e. CuCrO$_2$, the delafossite phase is thermally stable in air up to 1000 °C.

In this paper, the electrical properties of CuFe$_{1-x}$Cr$_x$O$_2$: Mg ($0 \leqslant x \leqslant 1$) solid solutions were studied by dielectric spectroscopy in order to observe the effect of the substitution of Fe by Cr on the M-site on the electrical conduction mechanism.

2. Experimental section

Polycrystalline samples of CuFe$_{1-x}$Cr$_x$O$_2$ ($0 \leqslant x \leqslant 1$) doped with 3% of Mg were prepared by a conventional solid-state reaction from stoichiometric mixtures of Cu$_2$O, Fe$_2$O$_3$, Cr$_2$O$_3$ and MgO commercial powders. Mg content is fixed to 3% in order to avoid the precipitation of the secondary phases [17]. The obtained mixtures were heated in a nitrogen atmosphere between 900 and 1000 °C for 30 h with intermittent grindings. Then, the powders were pressed into pellets and sintered at 1050 °C in neutral atmosphere for 10 h.

Electrical conductivity measurements were performed by recording the complex impedance $Z^*(\omega)$ and complex conductivity $\sigma^*(\omega)$ using a Novocontrol broadband dielectric spectrometer. The measurements were done in the frequency range from 10^{-2} to 10^6 Hz at room temperature and in the temperature range from -100 to 150 °C. The real part, $\sigma'(\omega)$, of the complex conductivity was investigated. The ac output voltage was adjusted to 1.5 V. For all the samples considered in this study, the phase lag between the measured impedance and the applied ac voltage was negligible at low frequencies, so that the reported impedance at 0.01 Hz is equivalent to the dc resistance. The dc conductivity σ_{dc} of samples was determined from the independent frequency part of $\sigma'(\omega)$ (low frequency plateau).

The powder samples were enclosed in a Teflon sample holder between two circular stainless steel electrodes (10 mm in diameter). The sintered samples 1.6 mm thick were placed between two circular gold platted electrodes (10 mm in diameter). To reduce contact resistance with the cell electrodes, a thin layer of gold (100 nm) was sputtered onto both sides of the pellets using a BOC Edwards scancoat six SEM sputter coater.

3. Results and discussion

3.1. Dc and ac conductivity

Figure 2 shows the frequency dependence of the real part, $\sigma'(\omega)$ of the complex electrical conductivity, for Mg-doped
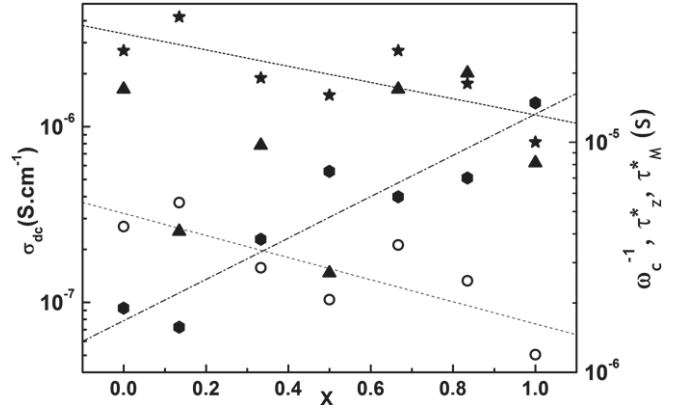
Table 1. Dc conductivity σ_{dc}, characteristic onset frequency ω_c and exponent n, using (1), for different $CuFe_{1-x}Cr_xO_2$ delafossite powders at room temperature.

	σ_{dc} (S cm^{-1})	ω_c (s^{-1})	n
$CuFeO_2$: Mg	9.3×10^{-8}	2.3×10^5	0.92
$CuFe_{0.835}Cr_{0.165}O_2$: Mg	7.2×10^{-8}	1.8×10^5	0.97
$CuFe_{0.667}Cr_{0.333}O_2$: Mg	2.3×10^{-7}	3.5×10^5	0.89
$CuFe_{0.5}Cr_{0.5}O_2$: Mg	5.6×10^{-7}	4.8×10^5	0.70
$CuFe_{0.333}Cr_{0.667}O_2$: Mg	4.0×10^{-7}	2.8×10^5	0.66
$CuFe_{0.165}Cr_{0.835}O_2$: Mg	5.1×10^{-7}	4.0×10^5	0.65
$CuCrO_2$: Mg	1.4×10^{-6}	8.4×10^5	0.64

Figure 3. x dependence of: (●) dc conductivity; (★) characteristic relaxation time τ_Z^* from impedance plot; (▲) characteristic relaxation time τ_M^* from dielectric modulus plot; (○) reciprocal characteristic onset frequency ω_c^{-1}.

$CuFe_{1-x}Cr_xO_2$ powders at room temperature (25 °C). At low frequencies, $\sigma'(\omega)$ is independent of the electric field frequency. Above a characteristic onset angular frequency ω_c, the ac conductivity increases with increasing angular frequency and obeys a power law. Then, the angular frequency dependence of the total ac conductivity is well described by the following equation:

$$\sigma'(\omega) = \sigma(0) + A\omega^n = \sigma_{dc}\left[1 + \left(\frac{\omega}{\omega_c}\right)^n\right], \quad (1)$$

where σ_{dc} is the independent frequency conductivity or dc conductivity, $A = \omega_c^{-n}\sigma_{dc}$ is a pre-exponential factor and n is an exponent dependent on both frequency and temperature in the range $0 < n \leqslant 1$. This behaviour is characteristics of the charge transport in disordered materials and interpreted by Jonscher [18] as universal dynamic response (UDR). However a value of $n > 1$ was reported in ion-conducting glasses [19], ionic crystals [20, 21] and underlined by Papathanassiou et al [22, 23] in a new approach of the universal power law in disordered materials. The experimental $\sigma'(\omega)$ conductivity for $CuFe_{1-x}Cr_xO_2$ powders were fitted using (1). The best fits of the conductivity spectra at room temperature for $0 \leqslant x \leqslant 1$ are shown as solid lines in figure 2. The dc conductivity σ_{dc}, the crossover frequency ω_c and the exponent n were obtained by a non-linear fitting procedure and reported in table 1. The variation of the dc conductivity with x is shown in figure 3. As expected the conductivity increases weakly with x, only one decade in magnitude, because the progressive substitution of Fe^{3+} by Cr^{3+} reduces the distance Cu^+–Cu^+ in $CuFe_{1-x}Cr_xO_2$. The inset in figure 3 shows the variation of the power law exponent n with x. The exponent n decreases from 0.92 for $CuFeO_2$ ($x = 0$) to 0.65 for $CuCrO_2$ ($x = 1$) and a sharp decrease is observed above $x = 0.5$. This behaviour can be compared with the decrease in particles sizes of $CuFe_{1-x}Cr_xO_2$ solid solution with increasing x [16]. The substitution of Fe^{3+} by Cr^{3+} leaded to contraction of unit cell, and reduction in lattice parameter a. The lower value of n above $x = 0.5$ indicates that the dispersion of ac conductivity with frequency is reduced with the introduction of large amount of Cr at the Fe site. This behaviour may be correlated with the change in the distance and barrier height of the sites available for charge carriers for electrical conduction. The decrease in the lattice parameter a in the plane of the Cu atoms and the increased overlap between Cu^+($3d^{10}$) with increasing x are responsible for the observed n decrease through a reinforcement of the interaction between Cu^+ ions.
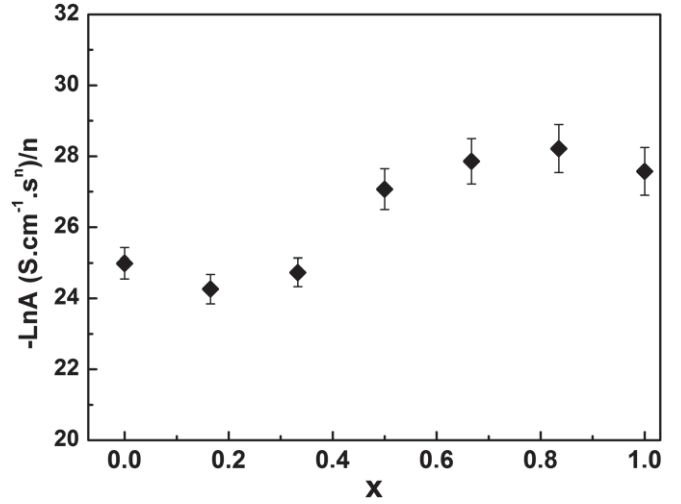
Figure 4. Composition dependence of the ratio $(-\text{Ln}A/n)$ in $CuFe_{1-x}Cr_xO_2$ delafossite at room temperature.

The ac conductivity is dependent on the stoichiometric parameter x as the dc conductivity and does not obey a scaling with x, i.e. no scaling law is obtained for all the $CuFe_{1-x}Cr_xO_2$ delafossite when the reduced conductivity $\sigma'(\omega)/\sigma_{dc}$ is plotted against the reduced frequency $\omega_r = a_x\omega$ where $a_x = [\omega(x)/\omega(x = 1)]$ is a shift factor depending on x, i.e. all the conductivity curves at constant x do not fall onto one master curve. The shape of the frequency dependence of the ac conductivity is then dependent on x as dc conductivity and the onset frequency.

According to the revision of the universal power law dispersion of ac conductivity in disordered solids proposed by Papathanassiou [22], the ratio $-\text{Ln}A/n$ is reported as a function of x in figure 4. This ratio is near constant because the weak change in the dc conductivity value with the substitution of Fe^{3+} by Cr^{3+}. Such behaviour, i.e. $-\text{Ln}A/n$ independent of composition, was observed in ion-conducting glasses [19].

The effect of Cr substitution on the conduction relaxation mechanism of $CuFe_{1-x}Cr_xO_2$ powder was also investigated by the complex impedance $Z^*(\omega)$ and complex dielectric modulus M^* (ω as a function of angular frequency and
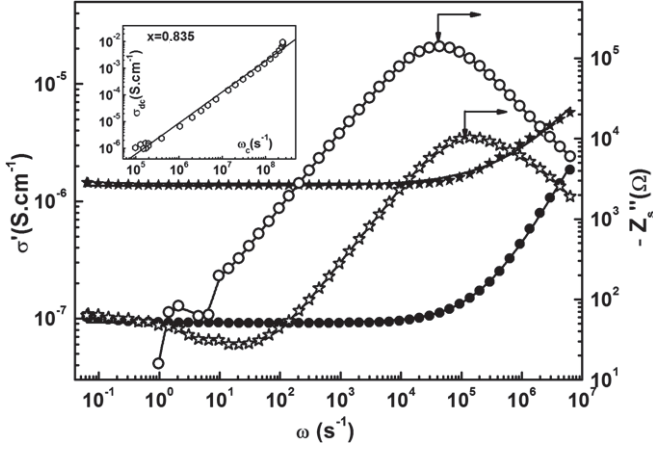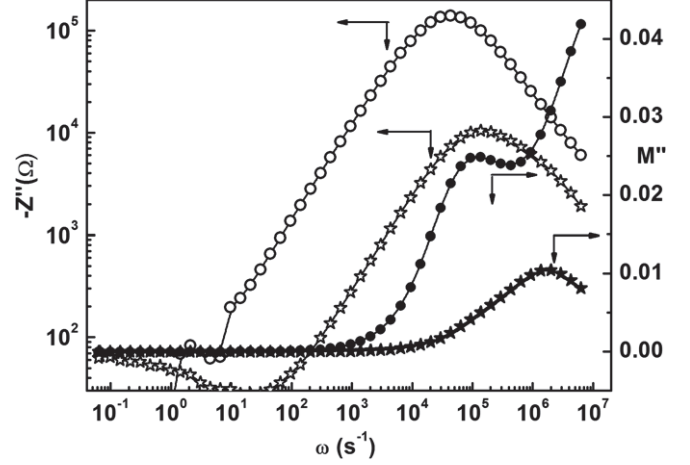
Figure 5. Angular frequency dependence of: the real part σ' of the complex conductivity for: ($\bullet$) $x = 0$; ($\bigstar$) $x = 1$ and the imaginary part Z_s'' of the complex impedance for: ($\bigcirc$) $x = 0$; ($\star$) $x = 1$. The inset shows the correlation between the characteristic onset frequency ω_c and the dc conductivity for $x = 0.335$. The solid line represents the least-squares linear fits to BNN relation (6).

Figure 6. Angular frequency dependence of: the imaginary part Z_s'' of the complex impedance for: ($\bigcirc$) $x = 0$; ($\star$) $x = 1$ and the imaginary part M'' of the complex dielectric modulus for: ($\bullet$) $x = 0$; ($\bigstar$) $x = 1$. Data points are connected to guide the eye.

temperature. Electrical modulus formalism was used in conductive materials to distinguish a frequency domain within the charge transport that is long range and above which is localized since it emphasizes bulk properties compared with the interfacial polarization. The frequency dependence of the imaginary part' of $Z^*(\omega)$, $Z''(\omega)$ is shown in figure 5 for $CuFeO_2$ ($x = 0$) to and $CuCrO_2$ ($x = 1$) and compared with the $\sigma'(\omega)$ behaviour. The relaxation conduction of charge carriers is represented by well-defined loss peaks in $Z''(\omega)$ and no such corresponding peak in the imaginary part of the complex dielectric permittivity $\varepsilon''(\omega)$ occurs. The maximum of the Z'' spectrum, occurring in the high frequency range part of the experimental frequency range $[10^{-2}–10^6$ Hz], is associated with the contribution of the bulk property of the material. Let τ_Z be the relaxation times obtained from the impedance plot. The absence of a ε'' loss peak together with the equivalence $\omega_c^{-1} \approx \tau_Z$ signify long range charge carriers diffusion. The conduction relaxation mechanism in $CuFe_{1-x}Cr_xO_2$ powder is also investigated by analysing electrical loss modulus M'' as a function of frequency and temperature. The imaginary part of modulus spectra is reported in figure 6 for $x = 0$ to and $x = 1$ and compared with Z'' spectra. The M'' spectrum exhibits one main peak as the Z'' spectrum. It is important to note that M'' maxima are at higher frequency with respect to Z'' maxima. Let τ_M be the relaxation times obtained from the modulus plot. The relatively large width and asymmetrical nature of the Z'' and M'' peaks at room temperature indicate a non-Debye behaviour of the conduction relaxation process. In order to follow the effect of the substitution of Fe^{3+} by Cr^{3+} on relaxation times, Havriliak–Negami (HN) empirical equation was used to describe the frequency dependence of the shape of the Z'' and M'' peaks as follows:

$$Z_s^* = Z_s' - \mathrm{i}\, Z_s'' = \frac{R_s}{[1 + (\mathrm{i}\omega\tau_Z^*)^\alpha]^\beta}, \tag{2}$$

$$M^* = M' + \mathrm{i}M'' = M_\infty - \frac{(M_\infty - M_0)}{[1 + (\mathrm{i}\omega\tau_M^*)^\alpha]^\beta}, \tag{3}$$

where τ_Z^* and τ_M^* are the HN characteristics relaxation time, and α and β the parameters describing the distribution of relaxation time. The parameters describing the conduction relaxation for the different $CuFe_{1-x}Cr_xO_2$ samples are listed in table 2. The variation of ω_c^{-1}, τ_Z^* and τ_M^* with x at room temperature is reported in figure 3. The three representations of the conduction relaxation show that the characteristics relaxation time decreases with increasing x. The magnitude of Z'' is founded to decrease as x increases, because R_s decreases. This result is in good agreement with the shortening of the distance between Cu sites as x increases.

The frequency behaviour of the ac conductivity at different temperatures for $x = 0.835$ is reported in figure 7. As expected for semiconductor behaviour, σ_{dc} increases with increasing temperature. Figure 8 displays the temperature dependence of the dc conductivity data in an Arrhenius plot for $x = 0.835$. The activation energy for the thermally activated conduction process is obtained by fitting the dc conductivity data with the Arrhenius relation:

$$\sigma_{dc} = \sigma_0 \exp\left(-\frac{E_\sigma}{k_B T}\right), \tag{4}$$

where σ_0 is the pre-exponential factor and E_σ is the activation energy for dc conductivity. As can be seen, only the data from $-30\,°C$ to about $150\,°C$ can be well linearized in this representation with $E_\sigma = 0.43$ eV and $\sigma_0 = 1905\,\mathrm{S\,cm^{-1}}$.

In the UDR the onset frequency or the crossover frequency ω_c from the dc regime at low frequencies to the dispersive regime is also the hopping frequency ω_h. The frequency behaviour of ac conductivity as a power law was largely observed in many other low mobility oxides amorphous semiconductors and disordered systems and attributed to the hopping of charge carriers between sites having variable heights and separation distances. To correlate dc and ac conductivities, the temperature dependence of the hopping frequency ω_h is compared with the corresponding dc conductivity behaviour in figure 8. As expected the

4

Table 2. Number density of Cu sites N_{Cu}, Cu–Cu distance (a-axis lattice parameter), number density of effective charge carrier density N_c using (8) and charge carrier mobility μ using (9) for different powders at room temperature.

	N_{Cu} (m^{-3})	a (Å) [16]	N_c (m^{-3})	μ(m^{-2} V^{-1} S^{-1})
CuFeO$_2$: Mg	2.19×10^{28}	3.0344	2.64×10^{27}	2.2×10^{-14}
CuFe$_{0.835}$Cr$_{0.165}$O$_2$: Mg	2.21×10^{28}	3.0268	2.65×10^{27}	1.7×10^{-14}
CuFe$_{0.667}$Cr$_{0.333}$O$_2$: Mg	2.22×10^{28}	3.0159	4.38×10^{27}	3.3×10^{-14}
CuFe$_{0.5}$Cr$_{0.5}$O$_2$: Mg	2.24×10^{28}	3.0055	7.82×10^{27}	4.5×10^{-14}
CuFe$_{0.333}$Cr$_{0.667}$O$_2$: Mg	2.26×10^{28}	2.9942	9.65×10^{27}	2.6×10^{-14}
CuFe$_{0.165}$Cr$_{0.835}$O$_2$: Mg	2.28×10^{28}	2.9826	8.68×10^{27}	3.7×10^{-14}
CuCrO$_2$: Mg	2.29×10^{28}	2.9742	1.14×10^{28}	7.7×10^{-14}
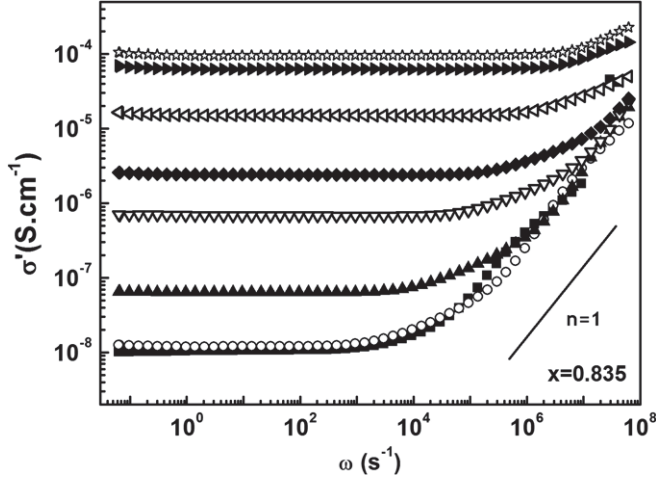
Figure 7. Angular frequency dependence of the real part σ' of the complex conductivity at different temperatures between −100 and 150 °C: (■) −100 °C; (○) −60 °C; (▲) −20 °C; (▽) 40 °C; (◆) 80 °C; (◁) 120 °C; (☆) 150 °C for $x = 0.835$.
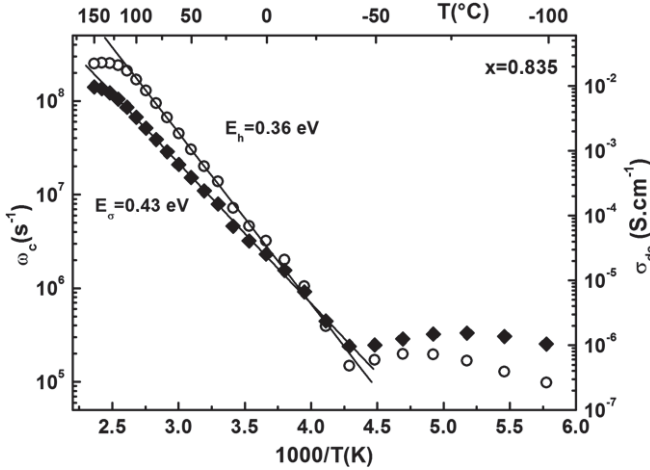
Figure 8. Dc conductivity σ_{dc} (◆) and characteristic onset frequency ω_c (○) as a function of reciprocal temperature for $x = 0.835$. Solids lines represent the fit of experimental data using (4) and (5).

crossover frequency is also thermally activated and ω_h obeys an Arrhenius equation:

$$\omega_c \equiv \omega_h = \omega_{h0} \exp\left(-\frac{E_h}{k_B T}\right) \tag{5}$$

with an activation energy value $E_h = 0.36$ eV close to the value of E_σ. The value of the corresponding characteristic hopping attempt frequency $\omega_{h0} = 10^{13}$ s^{-1} is close to the lattice phonon

frequency such as the inverse pre-exponential factor $1/\tau_{0Z,M}$. It is well known that, in most conductive materials, σ_{dc} and ω_h satisfy the Barton–Nakajima–Namikawa (BNN) relation [24–26], i.e.

$$\sigma_{dc} = p\varepsilon_0 \Delta\varepsilon\omega_c, \tag{6}$$

where p is a constant of order 1, $\Delta\varepsilon$ is the dielectric strength and ε_0 is the permittivity of free space. σ_{dc} and ω_h are thermally activated with nearly the same activation energy. The inset in figure 5 shows the log σ_{dc} versus log ω_h for $x = 0.5$. The solid line is the least-squares straight-line fit and gives a slope of 1.16 close to unity in good agreement with the BNN relation $\sigma_{dc} \sim \omega_h$. It can be concluded that dc and ac conductions are correlated with each other in CuFe$_{1-x}$Cr$_x$O$_2$ delafossite and that they are governed by the same transport mechanism, namely thermally activated nearest neighbour hopping.

At the lower temperature range, below −40 °C, the dc conductivity is independent of the temperature. The thermally activated behaviour for conduction in the temperature range [−30, 150 °C] is confirmed by analysing the temperature dependence of τ_Z^* and τ_M^*. It is clear that the relaxation times predicted by each empirical equation show an activated behaviour, i.e. obey the Arrhenius equation:

$$\tau_{z,M}^* = \tau_{0Z,M} \exp\left(\frac{E_{aZ,M}}{k_B T}\right), \tag{7}$$

where E_a is the activation energy and τ_0 is the high-temperature limit of the relaxation time. The best fit to (7) gives $E_{aZ} = 0.35$ eV and $E_{aM} = 0.39$ eV which corresponds to the value of dc conduction activation energy E_σ. This result indicates that charge carrier has to overcome the same energy barrier while conducting as well as relaxing. The mechanism of electrical conduction is the same as that of dielectric relaxation in CuFe$_{1-x}$Cr$_x$O$_2$ powder. As expected from the observed dc conductivity temperature behaviour, ω_c and τ_Z^* are independent of the temperature below −40 °C.

In hopping transport, we can use the relationship between the dc conductivity σ_{dc} and the hopping frequency ω_h [27],

$$\sigma_{dc} = \left(\frac{N_c e^2 r_h^2}{12\pi k_B T}\right)\omega_h, \tag{8}$$

where r_h is the hopping distance (i.e. the Cu–Cu distance a [16]) and N_c is the number density of effective charge carrier. Using (8), N_c can be evaluated at room temperature and compared with the number density of Cu sites in CuFe$_{1-x}$Cr$_x$O$_2$ delafossite. As shown in table 2, N_c increases
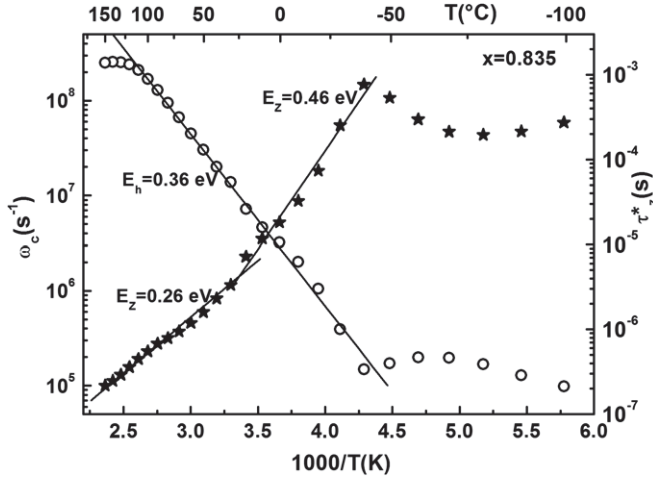
Figure 9. Characteristic onset frequency ω_c ($\circ$) and characteristic relaxation time τ_Z^* ($\star$) as a function of reciprocal temperature for $x = 0.835$. Solids lines represent the fit of experimental data using (5) and (7).
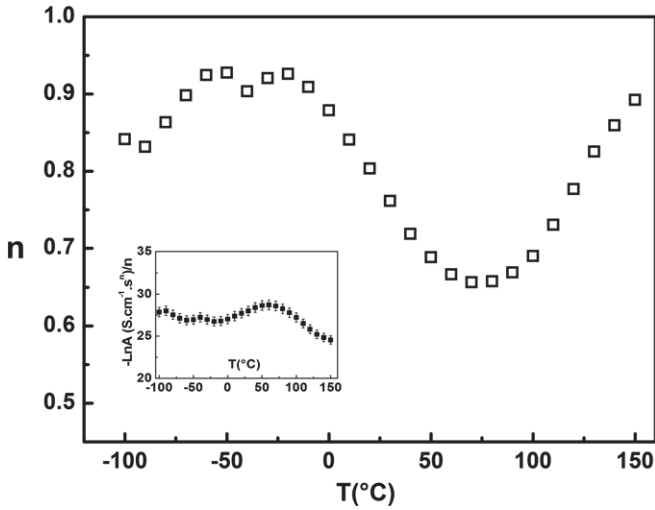
Figure 10. Variation of the exponent n with temperature for $x = 0.835$. The inset shows the temperature dependence of the ratio $(-\mathrm{Ln}\, A/n)$.

with x and the value is close to N_{Cu} for $CuCrO_2$ ($x = 1$) as expected, if one takes into account that the charge carrier hopping probability is necessarily reduced to some extent in the real delafossite powder. From σ_{dc} and N_c, the charge carrier mobility μ can be obtained using

$$\mu = \frac{\sigma_{dc}}{eN_c} \qquad (9)$$

and is reported in table 2.

To complete the temperature behaviour of ac conductivity, the temperature dependence of the frequency exponent n for $x = 0.835$ is shown in figure 9. The value of n calculated from (1) in figure 10 decreases with increasing temperature from -30 to $50\,°C$ and is increasing above $80\,°C$. The temperature dependence of n, at low temperature up to $-10\,°C$, is weak compared with the variation above $0\,°C$. This behaviour suggests that relaxation processes and conduction mechanism at low temperature are linked to tunnelling of charge carriers.

This result is in agreement with the weak activation energy measured below $-40\,°C$ using the temperature dependence of dc conductivity; impedance and loss modulus (see figures 8 and 9).

According to Dyre *et al* [28] presentation of a review on ac hopping conduction, the temperature dependence of the parameter n was explained on the basis of the many body interaction models. At low temperatures the interaction between the neighbouring charge carriers is almost negligible. As the temperature increases, the interaction increases, leading to a decrease in n. The universal power law dependence of ac conductivity on the frequency corresponds to the short range hopping of charge carriers between the sites separated by energy barriers of varied heights. If hopping takes place between a random distribution of localized charge states, it then lies between 0.5 and 1 as observed in $CuFe_{1-x}Cr_xO_2$ delafossite. The lower value of n occurs for multiple hops while the higher value occurs for single hops. Theoretical models have been proposed to correlate the conduction mechanism of ac conductivity with $n(T)$ behaviour. If n increases with temperature, a small polaron is the predominant mechanism, while the correlated barrier hopping (CBH) is characterized by a decrease in n with temperature [29]. Benko *et al* [2] assumed the conduction mechanism by hopping of small polarons localized on the Cu sites in Mg-doped $CuFeO_2$. Substituting Mg^{2+} for Fe^{3+} by Mg doping results in the mixed valence Cu^+/Cu^{2+} and contributes a hole. The calculated carrier mobility is very low and insufficient to measure the Seebeck coefficient in sample powders and to display some precise information about the nature of the involved charge carrier in the conduction of the $CuFe_{1-x}Cr_xO_2$ delafossite.

According to Papathanassiou [22] the ratio ($\mathrm{Ln}\, A/n$), in disordered solids, is independent of the temperature. The ratio $-\mathrm{Ln}\, A/n$ is reported as a function of temperature in the inset of figure 4. The variation of ($-\mathrm{Ln}\, A/n$) in delafossite ($x = 0.835$) is less than 2 orders of magnitude in the investigated temperature range. This behaviour is in agreement with those observed in other experimental data from ionic conducting glasses or disordered semiconductors and compiled by Papathanassiou [22].

From the literature, the conduction mechanism in $CuCrO_2$ [8, 30, 31] or $CuFeO_2$ delafossites at low temperature ($T < 25\,°C$) is a hopping of holes between the nearest neighbour Cu sites in Cu layers and a crossover from thermal activation behaviour to that of 3D VRH occurs at a very low temperature. As shown in figures 8 and 9, a such VRH behaviour of σ_{dc} in $T^{0.25}$ is not observed because σ_{dc}, τ_Z^* and ω_c are independent of the temperature below $-40\,°C$. Hence the charge carrier transport occurs via tunnelling from Cu atom to another at low temperature.

4. Conclusion

The electrical conductivity and dielectric behaviour of Mg-doped $CuFe_{1-x}Cr_xO_2$ delafossite powders have been studied by dielectric spectrometry. At room temperature, the conductivity behaviour is frequency and composition-dependent and obeys a power law, above the onset frequency

6

ω_c. In CuFe$_{1-x}$Cr$_x$O$_2$ delafossite no scaling of ac conductivity has been observed at room temperature at different x. The Cu$^+$–Cu$^+$ distance has a great influence on electrical properties of CuFe$_{1-x}$Cr$_x$O$_2$ delafossite. The dc conductivity σ_{dc} increases with increasing x and decreasing Cu–Cu distance. The behaviour of the exponent n in the power law shows also a decrease when x increases from 0 to 1. The dc and ac conductivities are driven by the same mechanism, as the BNN relation is found to be valid. The same temperature behaviour is observed for the dc conductivity and the onset frequency: the activation energy is the same for both ac and dc conduction, confirming the BNN relation. The dielectric behaviour of CuFe$_{1-x}$Cr$_x$O$_2$ delafossite powders has been analysed in the framework of complex impedance and complex dielectric modulus. The characteristic relaxation times τ_Z^* and τ_M^* extracted from impedance and modulus losses $Z''(\omega)$ and $M''(\omega)$, using a HN empirical equation, are decreasing monotonic functions of x in agreement with the x dependence of dc conductivity. The observed dielectric behaviour is characteristic of a conduction relaxation of charge carriers. Above $-40\,^\circ$C, the characteristic relaxation time τ_Z^* is thermally activated and the activation energy is close to the value obtained from dc conductivity for $x = 0.835$. The relaxation conduction and dc conduction are governed by charge carriers hopping from the Cu site to another. At low temperature, the charge transport occurs via tunnelling.

In delafossite, the ratio Ln A/n extracted from the power law dispersion of the ac conductivity was found to be poorly dependent on composition and temperature.

References

[1] Rogers D B, Shannon R D, Prewitt C T and Gillson J L 1971 *Inorg. Chem.* **10** 723
[2] Benko F A and Koffyberg F P 1984 *J. Phys. Chem. Solids* **45** 57
[3] Doumerc J P, Wichainchai A, Ammar A, Pouchard M and Hagenmuller P 1986 *Mater. Res. Bull.* **21** 745
[4] Kawazoe H, Yasukawa M, Hyodo H, Kurita M, Yanagi H and Hosono H 1997 *Nature* **389** 939
[5] Gong H, Wang Y and Luo Y 2000 *Appl. Phys. Lett.* **76** 3959
[6] Yanagi H, Inoue S I, Ueda K and Kawazoe H 2000 *J. Appl. Phys.* **88** 4159
[7] Jayaraj M K, Draeseke A D, Tate J and Sleight A W 2001 *Thin Solid Films* **397** 244
[8] Nagarajan R, Draeseke A D, Sleight A W and Tate J 2001 *J. Appl. Phys.* **89** 8022
[9] Nagarajan R, Duan N, Jayaraj M K, Li J, Vanaja K A, Yokochi A, Draeseke A, Tate J and Sleight A W 2001 *Int. J. Inorg. Mater.* **3** 265
[10] Benko F A and Koffyberg F P 1987 *J. Phys. Chem. Solids* **48** 431
[11] Nozaki T, Hayashi K and Kajitani T 2008 *Proc. ICT 2007 26th Int. Conf. on Thermoelectrics (Jeju Island, Korea, June 2007)* p 168
[12] Thomas G 1997 *Nature* **389** 907
[13] Ingram B J, Mason T O, Asahi R, Park K T and Freeman A J 2001 *Phys. Rev.* B **64** 155114
[14] Mugnier E, Barnabé A and Tailhades Ph 2006 *Solid State Ion.* **177** 607
[15] Barnabé A, Mugnier E, Presmanes L and Tailhades Ph 2006 *Mater. Lett.* **60** 3468
[16] Lalanne M, Barnabé A, Mathieu F and Tailhades Ph 2009 *Inorg. Chem.* **48** 6065
[17] Sadik P W, Ivill M, Craciun V and Norton D P 2009 *Thin Solid Films* **517** 3211
[18] Jonscher A K 1977 *Nature* **267** 673
[19] Cramer C, Brunklaus S, Ratai E and Gao Y 2003 *Phys. Rev. Lett.* **91** 26601
[20] Chen R H, Yang R Y and Shern S C 2002 *J. Phys. Chem. Solids* **63** 2069
[21] Louati B, Gargouri M, Guidara K and Mhiri T 2005 *J. Phys. Chem. Solids* **6** 762
[22] Papathanassiou A N 2005 *Mater. Lett.* **59** 1634
Papathanassiou A N 2006 *J Non-Cryst Solids* **352** 5444
[23] Papathanassiou A N, Sakellis I and Grammatikakis J 2007 *Appl. Phys. Lett.* **91** 122911
[24] Barton J L 1966 *Verres Refract.* **20** 328
[25] Nakajima T 1972 *Ann. Rep. Conf. on Electrical Insulation and Dielectric Phenomena* (Washington DC: National Academy of Sciences) p 168
[26] Namikawa H 1975 *J. Non-Cryst. Solids* **18** 173
[27] Mott N F and Davis E A 1979 *Electronic Processes in Non-crystalline Materials* (Oxford: Clarendon)
[28] Dyre J C and Schroder T B 2000 *Rev. Mod. Phys.* **72** 873
[29] Elliot S R 1977 *Phil. Mag.* **36** 1291
Elliot S R 1987 *Adv. Phys.* **36** 135
[30] Okuda T, Jufuku N, Hidaka S and Terada N 2005 *Phys. Rev.* B **72** 144403
[31] Li D, Fang X, Deng Z, Zhou S, Tao R, Dong W, Wang T, Zhao Y, Meng G and Zhu X 2007 *J. Phys. D: Appl. Phys.* **40** 4910